Timescales for detection of trends in the ocean carbon sink

Galen A. McKinley[1], Darren J. Pilcher[1,2], Amanda R. Fay[1], Keith Lindsay[3], Matthew C. Long[3], Nicole S. Lovenduski[4]

[1] University of Wisconsin – Madison, Department of Atmospheric and Oceanic Sciences and Center for Climatic Research, Madison, WI USA

[2] NOAA Pacific Marine Environmental Laboratory, Seattle, WA, USA

[3] National Center for Atmospheric Research, Boulder, CO, USA

[4] Department of Atmospheric and Oceanic Sciences and Institute of Arctic and Alpine Research, University of Colorado Boulder, Boulder, CO, USA

The ocean has accumulated 41% of all anthropogenic carbon emitted as a result of fossil fuel burning and cement manufacture[1,2]. The magnitude and the large-scale distribution of the ocean carbon sink is well quantified for recent decades[3,4]. In contrast, temporal changes in the oceanic carbon sink remain poorly understood[5,6,7]. It has proven difficult to distinguish between air-sea carbon flux trends due to anthropogenic climate change and those due to internal climate variability [5,6,8-13]. Here we use a modeling approach that allows for this separation[14], revealing how the ocean carbon sink may be expected to change throughout this century in different oceanic regions. Our findings suggest that, due to large internal climate variability, it is unlikely that changes in the rate of anthropogenic carbon uptake can be directly observed in most oceanic regions at present, but that this may become possible between 2020-2050 in some regions.

Recent observationally-based syntheses have quantified mean ocean carbon uptake and its spatial distribution[1,3,4,15] (Extended Data Fig 1). In addition, interior ocean observations analyzed under the assumption of constant ocean circulation suggest a steady increase in the integrated sink over the last century [1,15]. Yet surface observations clearly indicate that carbon uptake is strongly impacted by variability in surface climate and ocean circulation[5,8-13]. This variability impedes our ability to develop a detailed, regional picture of how the ocean carbon sink is changing in response to increasing atmospheric partial pressure of carbon dioxide (pCO_2) and the associated climate change. Though climate models suggest the ocean should be a net sink for anthropogenic carbon for at least the next several centuries, they also suggest that climate warming and circulation changes will act to reduce the sink's magnitude[7,16]. Monitoring current and future effects from the combined impact of increasing atmospheric pCO_2 and climate change, or the *forced trend,* on ocean carbon uptake presents a major observational challenge due to the strong influence of the variability inherent to the climate system [14,17-18].

Previous modeling studies have attempted to separate internal variability from forced trends in ocean carbon uptake using several approaches. Variability in air-sea carbon fluxes has been linked to modes of climate variability in realistic hindcast models[19-21]. However, anthropogenic change can project onto these modes, leading to an incomplete separation. The ocean's response to increasing atmospheric CO_2 in the absence of variability and change has been studied[13], but this approach ignores both mean impacts on ocean circulation from variable climate and indirect impacts on the carbon sink due to circulation change. Collections of Earth System Models have been used to assess relationships between natural variability and carbon cycle trends [22-23], but diverse model structures – for example, the spatial resolution of the atmosphere and ocean components, parameterization of the lower food web, or numerical schemes – can influence resulting trends[24]. Structural uncertainty precludes clear identification of the influence of internal variability[24].

We make use of a large ensemble of a single Earth System Model, the Community Earth System Model (CESM-LE, Ref. 25) to assess variability and change in the ocean carbon cycle in recent decades and through 2100. CESM is a comprehensive coupled climate model consisting of atmosphere, ocean, land surface, and sea ice components. The CESM-LE experiment includes 32 members with ocean biogeochemistry output. The experiment included a control integration of >2000 years. A transient integration (ensemble member 1) started at year 402 of the control and was integrated for 251 years under historical forcing (1850-2005) and then the Intergovernmental Panel on Climate Change Representative Concentration Pathway (IPCC RCP) 8.5 scenario for 2006-2100. Additional ensemble members were initialized from ensemble member 1 at January 1, 1920, with round-off level perturbations applied to the air temperature field. See Methods for more details.

Here, the use of a single model eliminates structural differences inherent to multi-model ensembles[24], allowing the spread across the ensemble to be wholly attributed to the internal variability of the modeled climate system[14,17-18,26]. For each ensemble member, temporal trends in any variable can be separated into two parts: (1) the *forced trend* that is common across all ensembles, and (2) the unforced, or *internal trend*, that occurs only in that ensemble member. The spread of trends across the ensemble indicates how much internal variability causes individual ensemble members to deviate from the forced trend[14,17-18,26]. The forced trend, as its name suggests, is due to the model forcing, here including anthropogenic greenhouse gases and aerosols, as well as natural forcings (e.g. solar variability and volcanoes) during the historical period[14,25]. In the case of the ocean carbon sink, there are two components to the forced trend. The first is the direct influence of increasing atmospheric $p$$CO_2$ driving continued ocean carbon uptake. The second is the indirect effect of changing climate that influences the physical state of the ocean and modulates air-sea carbon fluxes.

Comparisons to observations illustrate that CESM captures the dominant modes and magnitudes of ocean carbon cycle variability and trends at regional to global scales (Ref 21, Methods, Extended Data Tables 1 and 2). To further ground-truth the simulated mean CO_2 flux, we compare to fluxes estimated from observations[5], and to a multi-model ensemble of 12 Coupled Model Intercomparison Project 5 (CMIP5) Earth System Models (Fig 1, Extended Data Fig 1, Extended Data Table 3). For the 30-year mean CO_2 flux, CESM-LE is consistent with the observed estimates in most regions and for the global average, with small differences across the individual ensemble members (Fig 1). In contrast, there is a substantial spread in CO_2 flux estimates from CMIP5[23]. It can be expected that structural differences between models would dominate differences in the multi-decadal mean CO_2 flux, since the long averaging period integrates over the timescales of the dominant modes of variability. This is exactly what we find; a much greater spread in mean CO_2 flux for CMIP5 than CESM-LE for all biomes (Fig 1). These structural differences across CMIP5 also impact CO_2 flux trends (Methods, Extended Data Fig 2), indicating that a clean separation of forced trends from trends driven by internal variability is not possible with the CMIP5 multi-model ensemble as it is possible with CESM-LE.

Our model analysis considers forced trends and the spread of internal trends in the ocean carbon sink across timeframes from decadal to centennial, all starting in 1990. Forced trends are shown only if they can be distinguished from trends due to internal variability with 95% confidence[14] (Methods).

For the decade starting in 1990, internal variability is large enough to preclude identification of forced trends in the carbon sink across most of the ocean (Fig 2a). Internally-driven variability in trends (Fig 2d) is largest in the equatorial Pacific due to El Niño-Southern Oscillation effects, and in regions of strong seasonal and interannual climate variability, such as the high latitudes of the North Pacific and Atlantic and north of seasonal sea ice in the Southern Ocean [5,8,10,11,13,22,27,28]. Only in the subpolar North Atlantic, equatorial Atlantic and in some locations in the Southern Ocean are forced trends large enough to emerge from the variability over this period, and in these locations CO_2 uptake increases (Fig 2a).

Due to anthropogenic CO_2 emissions from 1990-2019, the ocean carbon sink increases in most locations outside the subtropics (Fig 2b). In isolated regions within the subtropics, the forced trend in carbon uptake for 1990-2019 is not large enough to be identifiable at the 95% level, despite the fact that internally-driven variability is substantially reduced relative to the decadal timeframe (Fig 2d,e). Over 100 years (1990-2089), anthropogenic forcing leads to strong increases in uptake in the high latitudes, and to reduced outgassing in the equatorial Pacific and the eastern upwelling zones off South America and Africa.

In the Pacific and Indian subtropics, the forced trend illustrates weakened carbon uptake by 2100 (Fig 2c). Internal variability has minimal impact on 100-year CO_2 flux trends (Fig 2f).

The ocean's capacity to absorb increasing amounts of anthropogenic CO_2 is not uniformly distributed. Across multi-decadal to centennial timescales, CO_2 flux does not change or decreases in the subtropical gyres (Fig 2b,c). This is consistent with a convergent large-scale circulation and strong stratification that isolates the surface from the deep ocean's large capacity to hold carbon. Long-term warming also reduces CO_2 solubility[10,13,16]. In contrast, the regions where ocean carbon uptake strongly increases are those with strong exchange between the surface and the deep ocean. In the equatorial Pacific, eastern boundary zones, and the Southern Ocean, upwelling deep waters have been out of contact with the atmosphere for hundreds of years and thus hold little, if any, anthropogenic carbon. As time progresses, upwelling waters encounter an ever-higher atmospheric pCO_2, which diminishes outgassing of natural carbon[4,22,28] (Extended Data Fig 1). In the North Atlantic, the direction of the exchange with the deep is reversed, with surface waters being transformed into deep waters by rapid buoyancy loss and deep convection. During this transformation, these waters increasingly absorb more carbon as atmospheric pCO_2 rises. There is large-scale correspondence of mean carbon uptake at present[3] and the regions predicted for uptake to grow most rapidly in the 21st century.

The ability to separate forced from internal trends in CESM-LE (Fig 2) allows for assessment of timescales over which observations would be required in order to detect anthropogenically-driven change in ocean carbon uptake from observations (Fig 3). Consistent with previous studies[26,29], detectability is assessed using Time of Emergence

(ToE), which is the year in which the signal of the forced trend would emerge from the noise of the internal variability. This analysis assumes observations began in 1990 (Methods).

The forced trend emerges early (by 2010) in some of the Southern Ocean and Atlantic where there is large short-term change in the sink. Given the strong internal variability and the smaller forced trend in the equatorial Pacific, ToE is generally intermediate here (by 2030 to 2050). The latest emergence occurs in the Pacific and Indian subtropical regions (2050+). Where the net effect of the forcing is to drive long-term steady carbon uptake, no change should be detected prior to 2100 (white in Fig 3). If internal variability were to be substantially underestimated or overestimated at a location, ToE estimates would be too short or too long, respectively. However, comparison to data indicates that CESM-LE reasonably captures carbon cycle variability (Extended Data Tables 1 and 2).

Based on our current observational system for surface ocean carbon, should we be able to detect these predicted changes? At seven ocean timeseries stations, direct measurements of the ocean carbon cycle have been made at quarterly to monthly intervals for one to several decades[9] (Fig 3). In the Atlantic, these locations are situated such that if observations had occurred since 1990 at a frequency sufficient to constrain the annual mean flux, they should be able to reveal change in the ocean carbon sink as distinct from internal variability at present (Irminger Sea, by 2015) or in the near future (BATS, ESTOC, CARIACO, by 2020; Iceland Sea, by 2040) (Fig 3). However, for the Pacific sites, detection of change in carbon uptake should not be expected until at least 2050 (HOT, by 2050; Munida, beyond 2100). Unfortunately, at the timeseries site where CESM-LE suggests the forced trend may be first detectable (Irminger Sea), the $p\mathrm{CO_2}$

dataset is short (1983-2005) and highly variable[9], making it impossible to determine if a trend toward increasing carbon flux is, in fact, occurring.

Surface ocean carbon data from volunteer commercial and scientific ships are presently too sparse for direct estimation of multi-decadal carbon cycle trends in most regions[5,8,10,12]. However, in the subtropics of the North Atlantic and Pacific, there are sufficient data to indicate a steady ocean carbon sink, and in the equatorial Atlantic to indicate an i□□□□□sing sink, for 1981-2009[10]. These changes are consistent with the 30-year forced signals expected from CESM-LE (Fig 2b). More data, from all sources, will be required to determine if these signals are, in fact, illustrating the forced trend in ocean carbon uptake[10].

Going forward, ocean carbon monitoring efforts can benefit from this new ability to separate internal variability from forced trends. Long-term records can be interpreted in the context of the expected forced change in the ocean carbon sink; monitoring can be targeted to regions where the largest forced changes are expected; and regional aggregation approaches that optimally seek the forced signal can be developed. Concurrently, expansion of these analyses to large ensembles of other Earth System Models[18,26] will further elucidate the mechanisms, magnitudes, and timescales of forced trends in the ocean carbon sink.

References

1. Khatiwala, S., Primeau, F., and Hall, T. Reconstruction of the history of anthropogenic CO_2 concentrations in the ocean. Nature 462, 2169–2191 (2009).
2. Ciais, P., and Sabine, C. Chapter 6: Carbon and Other Biogeochemical Cycles, in Climate Change. The Physical Science Basis. Contribution of Working Group I to the Fifth Assessment Report of the Intergovernmental Panel on Climate Change, edited by T. F. Stocker, D. Qin, G.-K. Plattner, M. M. B. Tignor, S. K. Allen, J. Boschung, A. Nauels, Y. Xia, V. Bex, and P. M. Midgley, p. 1535. (Cambridge University Press, Cambridge, United Kingdom and New York, NY, USA, 2013).
3. Gruber, N. et al. Oceanic sources, sinks, and transport of atmospheric CO_2. Global Biogeochem Cycles 23, GB1005 (2009).
4. Takahashi, T., et al., Climatological mean and decadal change in surface ocean pCO_2, and net sea–air CO_2 flux over the global oceans. Deep-Sea Research Part II 56, 554–577 (2009).
5. Landschützer, P. et al. The reinvigoration of the Southern Ocean carbon sink. Science 349, 1221–1224 (2015).
6. Schuster, U. et al. An assessment of the Atlantic and Arctic sea–air CO_2 fluxes, 1990–2009. Biogeosciences 10, 607–627 (2013).
7. Randerson, J. T. et al. Multicentury changes in ocean and land contributions to the climate-carbon feedback. Global Biogeochem Cycles 29, doi:10.1002/2014GB005079. (2015).
8. Munro, D. R. et al. Recent evidence for a strengthening CO_2 sink in the Southern Ocean from carbonate system measurements in the Drake Passage (2002-2015). Geophys Res Lett. doi:10.1002/2015GL065194 (2015).
9. Bates, N. et al. A Time-Series View of Changing Ocean Chemistry Due to Ocean Uptake of Anthropogenic CO_2 and Ocean Acidification. Oceanography 27, 126–141 (2014).
10. Fay, A. R., McKinley, G. A. Global trends in surface ocean pCO_2 from in situ data. Global Biogeochem Cycles 27, doi:10.1002/gbc.20051 (2013).
11. McKinley, G. A., Fay, A. R., Takahashi, T. & Metzl, N. Convergence of atmospheric and North Atlantic carbon dioxide trends on multidecadal timescales. Nature Geoscience 4, 606–610 (2011).
12. Le Quéré, C., Raupach, M. R., Canadell, J. G. & Al, G. M. E. Trends in the sources and sinks of carbon dioxide. Nature Geoscience 2, 831–836 (2009).
13. Le Quéré, C., Takahashi, T., Buitenhuis, E. T., Rödenbeck, C. & Sutherland, S. C. Impact of climate change and variability on the global oceanic sink of CO_2. Global Biogeochem Cycles 24, GB4007 (2010).
14. Deser, C., Phillips, A., Bourdette, V. & Teng, H. Uncertainty in climate change projections: the role of internal variability. Climate Dynamics 38, 527–546, doi:10.1007/s00382-010-0977-x (2012b).
15. DeVries, T. The oceanic anthropogenic CO_2 sink: Storage, air-sea fluxes, and transports over the industrial era. Global Biogeochem. 28, 631–647 doi:10.1002/2013GB004739. (2014).
16. Sarmiento, J. L. & LeQuéré, C. Oceanic carbon dioxide uptake in a model of century-scale global warming. Science 274, 1346–1350 (1996).
17. Deser, C., Knutti, R., Solomon, S. & Phillips, A. S. Communication of the role of natural variability in future North American climate. Nature Climate Change 2, 775–779, doi:10.1038/nclimate1562 (2012a).
18. Frölicher, T. L., Joos, F., Plattner, G.-K., Steinacher, M. & Doney, S. C. Natural variability and anthropogenic trends in oceanic oxygen in a coupled carbon cycle-climate model ensemble. Global Biogeochem Cy 23, GB1003 (2009).
19. Ullman, D. J., McKinley, G. A., Bennington, V. & Dutkiewicz, S. Trends in the North Atlantic carbon sink: 1992–2006. Global Biogeochem Cycles 23, GB4011 (2009).
20. Lovenduski, N. & Gruber, N. Toward a mechanistic understanding of the decadal trends in the Southern Ocean carbon sink. Global Biogeochem Cycles 22, GB3016 (2008).
21. Long, M. C., Lindsay, K., Peacock, S., Moore, J. K. & Doney, S. C. Twentieth-century oceanic carbon uptake and storage in CESM1 (BGC). J Climate 26.18, 6775-6800 (2013).
22. Resplandy, L., Séférian, R. & Bopp, L. Natural variability of CO_2 and O_2 fluxes: What can we learn from centuries-long climate models simulations? J Geophys Res-Oceans 120, 384–404 (2015).

23. Frölicher, T. L. et al. Dominance of the Southern Ocean in Anthropogenic Carbon and Heat Uptake in CMIP5 Models. Journal of Climate 28, 862–886 (2015).
24. Hawkins, E. & Sutton, R. The potential to narrow uncertainty in regional climate predictions. Bulletin Of The American Meteorological Society 90, 1095–1107 (2009).
25. Kay, J. E., et al. The Community Earth System Model (CESM) Large Ensemble Project: A community resource for studying climate change in the presence of internal climate variability. Bulletin of the American Meteorological Society (2014).
26. Rodgers, K. B., Lin, J. & Frolicher, T. L. Emergence of multiple ocean ecosystem drivers in a large ensemble suite with an earth system model. Biogeosciences 12, 3301–3320 (2015).
27. Lovenduski, N.S., Fay, A.R., McKinley, G.A. Observing multi-decadal trends in Southern Ocean CO_2 uptake: What can we learn from an ocean model? Global Biogeochem Cycles 29, 416-426 (2015).
28. Landschützer, P., Gruber, N., Bakker, D. C. E. & Schuster, U. Recent variability of the global ocean carbon sink. Global Biogeochem Cycles 28, 927–949 (2014).
29. Hawkins, E. & Sutton, R. Time of emergence of climate signals. Geophys Res Lett 39, L01702 (2012).

Acknowledgements The National Science Foundation sponsors NCAR where CESM is developed. Computing resources were provided by the Climate Simulation Laboratory at NCAR's Computational and Information Systems Laboratory (CISL), sponsored by NSF and other agencies. NCAR's Advanced Study Program sponsored D.J.P., K.L., M.C.L. and G.A.M. to initiate this analysis. NASA (NNX11AF53G, NNX13AC53G) is thanked for funding for G.A.M., D.J.P., A.R.F., and N.S.L. N.S.L. also thanks NSF (OCE-1155240) and NOAA (NA12OAR4310058).

Author Contributions G.A.M. conceived of the analysis, which was further refined by all authors. K.L. coordinated inclusion of ocean biogeochemistry in CESM-LE. D.J.P. and A.R.F. did the analysis. All authors discussed results and contributed to writing the manuscript.

Author Information Reprints and permissions information is available at www.nature.com/reprints. The authors declare no competing financial interests. Readers are encouraged to comment on the online version of the paper. Correspondence and requests for materials should be addressed to G.A.M. (gamckinley@wisc.edu).

Figure 1. Modeled and observed mean 1982-2011 CO_2 flux in 15 ocean biomes (molC/m^2/yr): CESM-LE mean (X), max/min in gray (N=32). Color dot for CMIP5 models (N=12); biome colors on map (ICE, dark blue; SPSS, light blue; STSS, green; STPS, yellow; EQ, orange and red; full names in Extended Data Table 4; CESM-LE symbol aligns with line to indicate biome). Insufficient data in northern hemisphere ICE biomes[28]. Atlantic offset by -3 molC/m^2/yr, Southern and Indian by +3 molC/m^2/yr. Global mean (bottom right inset) with scale twice main figure; uncertainty on observed (gray band) is 0.12 molC/m^2/yr (Ref 28, personal communication).

Figure 2. Forced trends and internal variability of CESM-LE trends in sea-to-air CO_2 flux (molC/m^2/yr^2). Forced trends for **a** 1990-1999, **b** 1990-2019 and **c** 1990-2089. Gray is where the forced trend cannot be identified with 95% confidence (Methods). CO_2 flux trend standard deviations, indicating the impact of internal variability on CO_2 flux trends, for **d** 1990-1999, **e** 1990-2019, **f** 1990-2089. Negative indicates increasing ocean carbon uptake.

Figure 3: Time of Emergence for sea-to-air CO_2 flux. ToE is when the forced trend becomes detectable given the internal variability (Methods). Blue stars indicate seven ocean timeseries stations[9], from North to South in the Atlantic: 1. Iceland Sea, 2. Irminger Sea, 3. Bermuda Atlantic Time-series Study (BATS), 4. European Station for Time series in the Ocean at the Canary Islands (ESTOC), 5. Carbon Retention In A Colored Ocean (CARIACO) and from North to South in the Pacific, 6. Hawaii Ocean Time-series (HOT) and 7. Munida. Biome-mean ToEs are presented in Extended Data Table 4.

Methods

The Large Ensemble of the Community Earth System Model. The Community Earth System Model (CESM) is a comprehensive coupled climate model consisting of atmosphere, ocean, land, and sea ice component models[30]. The ocean physical model is the ocean component of the Community Climate System Model version 4[31]. The model has nominal 1^{o} horizontal resolution and 60 vertical levels. Mesoscale eddy transport, diapycnal mixing, mixed layer restratification by submesoscale eddies are parameterized with state-of-the-art approaches. The biogeochemical-ecosystem ocean model includes multi-nutrient co-limitation on phytoplankton growth and specific phytoplankton functional groups as well as full-depth ocean carbonate system thermodynamics, sea-air CO_2 fluxes, and a dynamic iron cycle[30]. The biogeochemical-ecosystem model compares favorably to observations, though there are some important biases including weak Southern Ocean CO_2 uptake[21].

The CESM-LE began with a multi-century 1850 control simulation with constant pre-industrial forcing; the ocean physical state was initialized from observations, ocean biogeochemical tracers were initialized from a separate 600-year spin up, and other component models were initialized from previous CESM1 simulations. Once the control simulation climate achieved quasi-equilibrium with the 1850 forcing, the first ensemble member was initialized from a randomly selected year in the 1850 control run: January 1, model year 402. Ensemble member 1 was integrated forward from 1850 to 2100. The remaining ensemble members were integrated from 1920 to 2100 using slightly different initial conditions: Ensemble member 2 used one-day lagged ocean initial conditions, while spread in the remaining ensemble members was generated by round-off level perturbations to their initial air temperature fields[25]. After initial condition memory was lost, each ensemble member evolved chaotically. A total of 38 ensemble members were generated in this fashion, but 6 of these had corrupted ocean biogeochemical output due to a setup error and affected fields were discarded. All ensemble members have the same specified external forcing: historical forcing from 1920 to 2005, and Representative Concentration Pathway (RCP) 8.5 forcing from 2006 to 2100. Differences from observed atmospheric $p$$CO_2$ for RCP8.5 for the 2006-2014 period are minimal[32]. Since atmospheric CO_2 concentrations are prescribed, CESM-LE ocean carbon fluxes do not feedback on the modeled climate.

Analysis methods. We consider the linear trend at each model gridcell of annual mean CO_2 flux, in units of molC/m^2/yr^2. The trend for CO_2 flux is calculated for each ensemble member. The *forced trend* is the average trend across the 32 ensembles. Each ensemble member's *internal trend,* due to internal variability, is the difference between that ensemble's trend and the forced trend. The 95% confidence level for identification of the forced trend is calculated, for each gridcell and timeframe, based on the number of ensembles required to resolve the ensemble mean response: $N_{min} = 8/(X/\sigma)^2$, where X is the forced trend and σ is the standard deviation of trends[14]. If N_{min} exceeds the number of ensembles in CESM-LE ($N_{ensembles}$ = 32), the forced trend cannot be identified with 95% confidence. Time of Emergence (ToE) is the first year in which the signal-to-noise ratio (S/N) exceeds a threshold value of 2, where the signal is the forced trend and the noise is the ensemble standard deviation[29]. For efficiency of computation and presentation, S/N ratios are calculated at 5-year intervals (i.e. 1990-1995, 1990-2000, 1990-2005, etc.). S/N must remain greater than 2 for all subsequent years.

Model comparisons to observations. To assess the representation of internal variability in CESM-LE, Extended Data Table 1 compares CESM-LE modeled to observed variability in annual mean pCO$_2$ and CO_2 flux for 1982-2011, and Extended Data Table 2 compares trends over the same period. pCO$_2$ data are from the Surface Ocean CO_2 Atlas (SOCATv2)[33] averaged to monthly means at 1x1 degree resolution. CESM-LE members are each sampled in pCO$_2$ to reflect the data density available in SOCATv2. A background mean climatology[4] is removed at 1x1 degree resolution in order to address the potential of spatial aliasing when averaging to biome-scale[10,34,35]. An area-weighted average is then used to arrive at biome scale annual means, and the 30-year trend is removed before calculating the standard deviation. For the CO_2 flux, we utilize monthly 1x1 degree resolution flux estimates that have full spatial and temporal coverage over the period 1982-2011[28]. These estimates are based on the same pCO$_2$ dataset (SOCATv2). With the full global coverage of the CO_2 flux product, there is no need to sample or to remove a background climatology from CESM-LE prior to biome averaging. Otherwise, the same processing is employed as for pCO$_2$. The uncertainty reported in Extended Data Table 1 is one standard deviation of the variability represented by the 32 CESM-LE members for each variable. There is insufficient data to make an independent uncertainty estimate with respect to variability from the observations. In Extended Data Table 2, linear trends in observed annual mean pCO$_2$ and CESM-LE pCO$_2$, sampled as these observations, are compared. Sampling as the observations allows for a direct model to observation comparison in spite of the fact that the sparse data coverage may lead to inaccurate observed estimates of annual mean pCO_2 for some biomes in some years. As in Extended Data Table 1, since the CO_2 flux product offers full coverage in space and time, there is no need for sampling.

Within the uncertainty, modeled pCO_2 variance is correct in seven of the biomes, underestimated in 5 biomes and overestimated in 3 biomes (Extended Data Table 1). However, in two of the three biomes where pCO_2 variability is overestimated by the model (SO STSS, SO SPSS), comparison to the CO_2 flux product suggests the model underestimates variability. In the third (NP STPS), the flux product comparison indicates that model appropriately simulates variability. Conversely, in the biomes where pCO_2 variability is underestimated, the CO_2 flux product comparison indicates either variability consistent with observations (NA STSS, EQ Atl), too high (NP STSS), or too low (NA SPSS, SA STPS). Similarly, in the biomes where pCO_2 variability is consistent with the observations, the CO_2 flux comparison indicates overestimation by the model (East EQ Pac, West EQ Pac, IND STPS), underestimation (NP SPSS, SO ICE), or consistency (SP STPS).

Modeled trends in pCO_2 and CO_2 flux (Extended Data Table 2) are largely consistent with observed trends, given the uncertainty. In one biome (West EQ Pac), the trend in pCO_2 in the model is overestimated, though in this biome the CO_2 flux trend is consistent with the observed estimates. In three biomes (NP STPS, East EQ Pac, IND STPS), the flux trend is too large, and in one (SO SPSS), it is too small. However, in all four of these biomes, the pCO_2 trends are consistent with the observed estimates. There is no clear relationship between over- and underestimation of trends and over- and underestimation of variability (Extended Data Table 1).

In the CESM-LE, pCO_2 variability and trends dominantly control CO_2 flux variability and trends[21]. Thus, the fact that these comparisons for pCO_2 and CO_2 flux variability and trends differ significantly suggests that there is additional, unquantified uncertainty driven by the sparse sampling for pCO_2 and assumptions made in the development of the flux product[28]. That CESM-LE falls clearly within the range of observed pCO_2 and estimated CO_2 flux variability and trends indicates that the model's representation of the carbon cycle is, on the whole, consistent with our current observational understanding. More observations are needed to better constrain internal variability and trends in the surface ocean carbon cycle.

Forced trends in the CMIP5 ensemble. Twelve CMIP5 earth system models are included in the analysis in addition to the CESM-LE for the historical period. The included CMIP5 models are those models that report CO_2 flux at monthly timescales for a historical simulation through 2005 and with the RCP8.5 scenario for 2006-2100; see Extended Data Table 3 for included models. The CESM1-BGC model included in the CMIP5 model suite is a predecessor to the CESM-LE.

Due to the combined effect of a smaller number of ensemble members for CMIP5 and the larger variability across these ensembles (Extended Data Fig 2d-f), due in part to structural differences[29], the forced trend in CO_2 flux cannot be identified from CMIP5 across in most of the global oceans, even for the timeframe 1990-2089 (Extended Data Fig 2a-c). Where the forced trend from CMIP5 is discernable, primarily in the equatorial Pacific and Southern Ocean, it is of the same sign as CESM-LE (increasing uptake) but of weaker magnitude.

Data sources. Surface Ocean CO_2 Atlas (SOCAT v2) $p\mathrm{CO_2}$ (Ref 33, www.socat.info/access.html). CO_2 flux estimates (Ref 28, http://cdiac.esd.ornl.gov/oceans/SPCO2_1982_2011_ETH_SOM_FFN.html).

Model output sources. CESM LE (Ref. 25, https://www.earthsystemgrid.org/dataset/ucar.cgd.ccsm4.CESM_CAM5_BGC_LE.html). CMIP5 (Ref 36, historical files: http://cerawww.dkrz.de/WDCC/ui/Compact.jsp?acronym=ETHhi; doi:10.1594/WDCC/ETHhi; RCP8.5 files: http://cerawww.dkrz.de/WDCC/ui/Compact.jsp?acronym=ETHr8; doi: 10.1594/WDCC/ETHr8).

Code availability. Codes for analysis and production of figures can be made available upon request. Please contact G.A.M. (gamckinley@wisc.edu).

30. Hurrell, J. W., et al. The community earth system model: A framework for collaborative research. Bulletin of the American Meteorological Society 94.9, 1339-1360 (2013).

31. Moore, J.K. et al. Marine ecosystem dynamics and biogeochemical cycling in the Community Earth System Model [CESM1 (BGC)]: Comparison of the 1990s with the 2090s under the RCP4.5 and RCP8.5 scenarios. J Climate, 26(23) 9291-9312 (2013).
32. Danabasoglu, G., S. C. Bates, B. P. Briegleb, S. R. Jayne, M. Jochum, W. G. Large, S. Peacock, and S. G. Yeager, The CCSM4 Ocean Component. J. Climate, 25 (5), 1361–1389, doi:10.1175/JCLI- D-11-00091.1 (2012).Bakker, D. C. E. et al. An update to the Surface Ocean CO_2 Atlas (SOCAT version 2), Earth System Science Data, 6, 69–90, doi:10.5194/essd-6-69-2014 (2014).
33. Fay, A. R., and McKinley, G. A. Global open-ocean biomes: mean and temporal variability. Earth Sys. Sci. Data, 6, 273-284, doi:10.5194/essd-6-273-2014 (2014).
34. Fay, A. R., McKinley, G. A., and Lovenduski, N. S. Southern Ocean carbon trends: Sensitivity to methods. Geophys. Res. Lett., 41(19), 6833-6840 (2014).
35. Taylor, K.E., R.J. Stouffer and G.A. Meehl: An Overview of CMIP5 and the experiment design. Bull. Amer. Meteor. Soc. 93, 485-498, doi:10.1175/BAMS-D-11-00094.1 (2012).
36. Chylek, P., Li, J., Dubey, M. K., Wang, M., and Lesins, G. Observed and model simulated 20th century Arctic temperature variability: Canadian Earth System Model CanESM2, Atmos. Chem. Phys. Discuss. 11, 22893-22907 (2011).
37. Collins, W. J., et al. Development and evaluation of an Earth-system model – HadGEM2, Geoscientific Model Development 4.4 1051-1075 (2011).
38. Dufresne, J-L., et al. Climate change projections using the IPSL-CM5 Earth System Model: from CMIP3 to CMIP5. Clim. Dyn. 40, no. 9-10, 2123-2165 (2013).
39. Dunne, J. P., et al. GFDL's ESM2 global coupled climate-carbon Earth System Models Part I: Physical formulation and baseline simulation characteristics. J. Climate 25 6646-6665 (2012).
40. Fogli, P. G., et al. INGV-CMCC carbon (ICC): a carbon cycle earth system model. CMCC Research Paper 61 (2009).
41. Giorgetta, M., et al. CMIP5 Simulations of the Max Planck Institute for Meteorology (MPI-M) Based on the MPI-ESM-LR Model: The Historical Experiment, Served by ESGF, World Data Cent. for Clim. (2012a).
42. Giorgetta, M., et al. CMIP5 Simulations of the Max Planck Institute for Meteorology (MPI-M) Based on the MPI-ESM-LR Model: The RCP85 Experiment, Served by ESGF, World Data Cent. for Clim. (2012b).
43. Ji, D., L. Wang, J. Feng, Q. Wu, H. Cheng, Q. Zhang, J. Yang, W. Dong, Y. Dai, D. Gong, R.-H. Zhang, X. Wang, J. Liu, J. C. Moore, D. Chen, and M. Zhou. Description and basic evaluation of Beijing Normal University Earth System Model (BNU-ESM) version 1. Geosci. Model Dev., 7, 2039–2064 (2014).
44. Lindsay, K., et al. Preindustrial-control and twentieth-century carbon cycle experiments with the Earth System Model CESM1 (BGC). J. Climate 27.24 8981-9005 (2014).
45. Tjiputra J. F., et al..Evaluation of the carbon cycle components in the Norwegian Earth System Model (NorESM), Geosci. Model Dev. 6, 301-325 (2012).
46. Volodin E. M., Dianskii, N. A. and Gusev, A. V. Simulating Present-Day Climate with the INMCM4.0 Coupled Model of the Atmospheric and Oceanic General Circulations. Izvestiya, Atmospheric and Oceanic Physics 46, 414-431 (2010).
47. Watanabe, S., et al. MIROC-ESM 2010: model description and basic results of CMIP5-20c3m experiments, Geosci. Model Dev., 4, 845-872 (2011).
48. Wu, T. et al. Global carbon budgets simulated by the Beijing Climate Center Climate System Model for the last century, J. Geophys. Res. Atmos. 118, 4336-4347 doi:10.1002/jgrd.50320 (2013).

For Extended_pg1.jpg

Extended Data Figure 1. Comparison of 1982-2011 mean CO_2 flux (molC/m^2/yr). a Data-based climatology (ref 28), **b** CESM large ensemble 32-member mean, and **c** mean of 12 CMIP5 models.

For Extended_pg2.jpg

Extended Data Figure 2. Forced trends and variability of CMIP5 trends in sea-to-air CO_2 flux (molC/m^2/yr^2). Forced trends for **a** 1990-1999, **b** 1990-2019 and **c** 1990-2089. Gray is where the forced trend cannot be distinguished from the variability with 95% confidence (Methods). CO_2 flux trend standard deviations, indicating the impact of variability on CO_2 flux trends, for **d** 1990-1999, **e** 1990-2019, **f** 1990-2089. Negative indicates increasing ocean carbon uptake.

For Extended_pg3.jpg

Extended Data Table 1 | Comparison of observed and modeled *p*CO_2 and CO_2 flux variability for 1982-2011

FOOTNOTE to Extended Data Table 1: Variability is the standard deviation of the annual means from 1982-2011. Uncertainty of the variability is the standard deviation of the variability estimates for each of the 32 CESM-LE ensemble members. Underline indicates that the modeled variability is lower than the observed variability, and italics indicates that modeled variability is higher than observed variability, in both cases taking into account the model-estimated uncertainty. $p\mathrm{CO_2}$ data is from ref 33, CO_2 flux data from ref 28.

For Extended_pg4.jpg

Extended Data Table 2 | Comparison of observed and modeled $p\mathrm{CO_2}$ and CO_2 flux trends for 1982-2011

FOOTNOTE to Extended Data Table 2: Underline indicates that the modeled trend is lower than the observed trend, and italics indicate that modeled trend is higher than observed trend, given the uncertainty (95% trend confidence intervals). Trends are based on annual means. $p\mathrm{CO_2}$ data is from ref 33, CO_2 flux data from ref 28.

For Extended_pg5.jpg

Extended Data Table 3 | CMIP5 models used

For Extended_pg6.jpg

Extended Data Table 4 | Biome long names (ref 34) and mean Time of Emergence

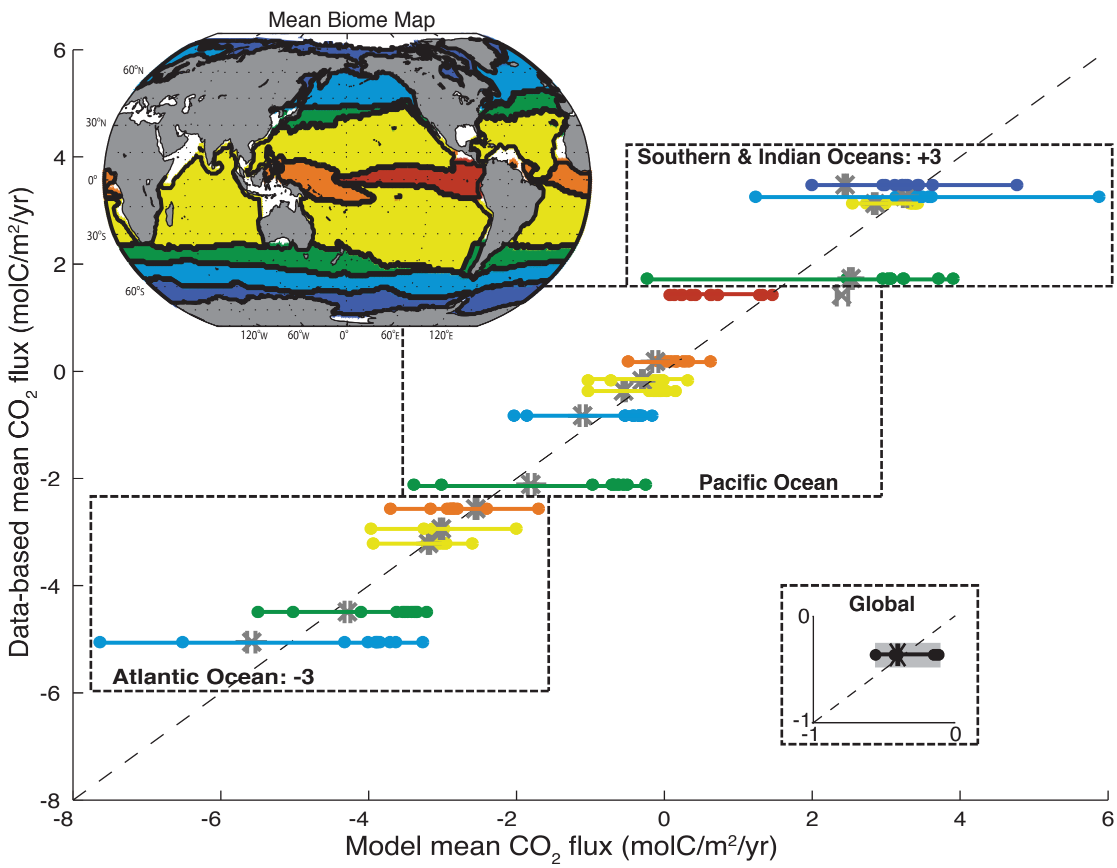

Mean Biome Map
60°N
30°N
0°
30°S
60°S
120°W
60°W
0°
60°E
120°E
Southern & Indian Oceans: +3
Pacific Ocean
Atlantic Ocean: -3
Global
0
-1
-1
0
6
4
2
0
-2
-4
-6
-8
-8
-6
-4
-2
0
2
4
6
Data-based mean CO_2 flux (molC/m^2/yr)
Model mean CO_2 flux (molC/m^2/yr)

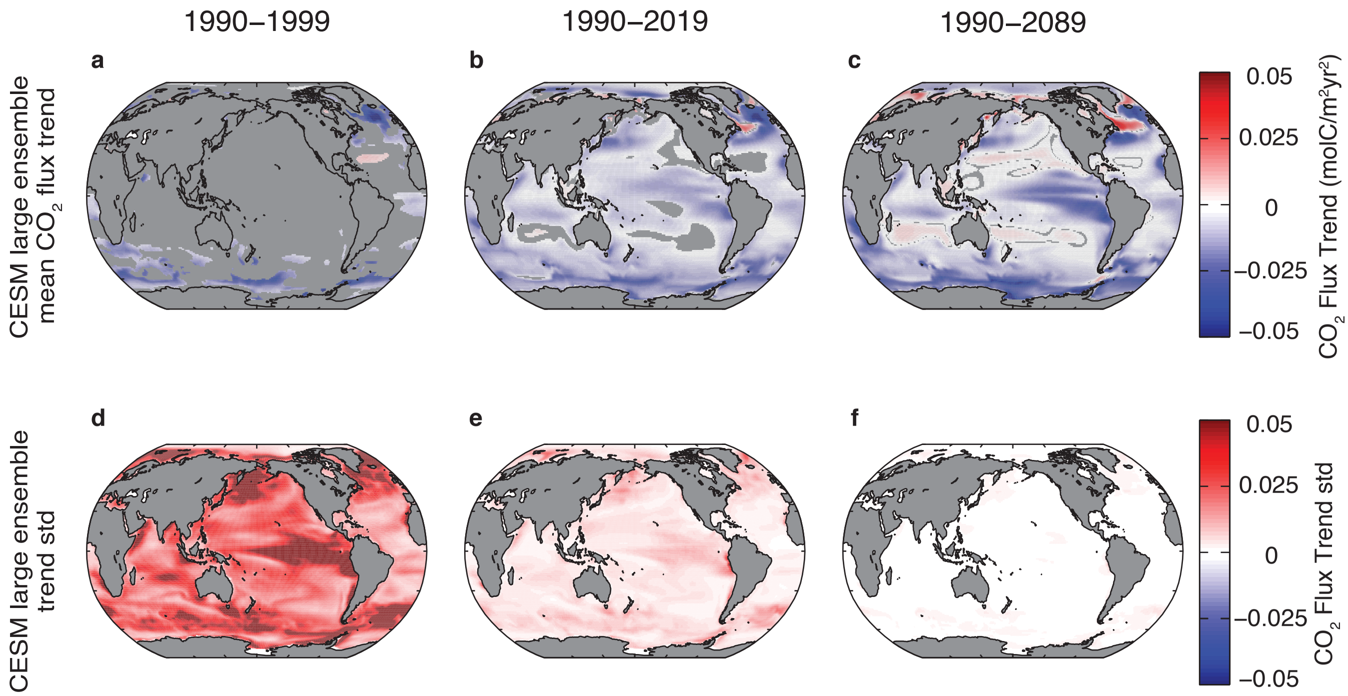

1990–1999
1990–2019
1990–2089
CESM large ensemble mean CO_2 flux trend
CESM large ensemble trend std
a
b
c
d
e
f
0.05
0.025
0
−0.025
−0.05
CO_2 Flux Trend (molC/m²yr²)
0.05
0.025
0
−0.025
−0.05
CO_2 Flux Trend std

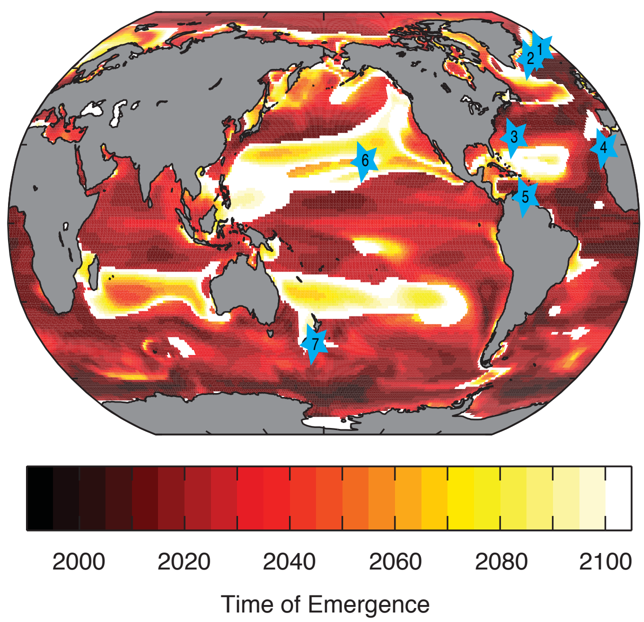
1
2
3
4
5
6
7
2000
2020
2040
2060
2080
2100
Time of Emergence

Supplementary Information for

Detectability of change in the ocean carbon sink

Galen A. McKinley, Darren J. Pilcher, Amanda R. Fay, Keith Lindsay,

Matthew C. Long, Nicole S. Lovenduski

Supplementary Methods

To assess the representation of internal variability in CESM-LE, Supplementary Table 1 compares CESM-LE modeled to observed standard deviations in 1982-2011 annual mean pCO_2 and CO_2 flux. The pCO_2 data are from the SOCATv2 dataset[31] averaged to monthly means at 1x1 degree resolution. The CESM LE members are each sampled in pCO_2 to reflect the data density available in SOCATv2. A background mean climatology[4] is removed at 1x1 degree resolution in order to address the potential of spatial aliasing when averaging to biome-scale means[12,32,33]. The datasets are then area-weighted average to biome scale annual means. The 30-year timeseries for each biome is detrended before calculating a standard deviation over the annual means.

For the CO_2 flux, we utilize monthly 1x1 degree resolution flux estimates that have full spatial and temporal coverage over the period 1982-2011 from (Ref 26, available at http://cdiac.esd.ornl.gov/oceans/SPCO2_1982_2011_ETH_SOM_FFN.html). These estimates are based on the same dataset used for the pCO_2 calculations (SOCATv2). With the full global coverage of the CO_2 flux product, there is no need to sample or to remove a background climatology from the CESM LE members prior to biome averaging and calculation of the flux standard deviation calculation. Otherwise, the same processing (area-weighted average to biome scale annual means, detrend, calculate annual standard deviation) is employed.

The uncertainty reported in Table S1 for each variable and each biome is one standard deviation of the variability represented by the 32 CESM-LE members for the respective variable (pCO_2 or CO_2 flux). There is insufficient data to make an independent uncertainty estimate from the observations.

Comparison and interpretation of observations and model internal variability is presented in Supplementary Discussion.

Supplementary Table 1: Annual mean pCO_2 and CO_2 Flux standard deviations and uncertainty in the standard deviations for 1982-2011. Blue shading indicates that the modeled variability is lower than the observed variability, and red shading indicates that modeled variability is higher than observed variability, in both cases taking into account the uncertainty bounds for both the modeled and observed estimates.

Biome	SOCAT pCO_2 std (μatm)	CESM-LE mean std (μatm)	Uncertainty (μatm)	Data-based Flux std (mol/m^2/yr)	CESM-LE mean std (mol/m^2/yr)	Uncertainty (mol/m^2/yr)
NP SPSS	7.9	10.2	2.0	0.42	0.13	0.02
NP STSS	7.3	5.9	0.4	0.09	0.13	0.01
NP STPS	4.2	5.4	0.5	0.05	0.07	0.01
East EQ Pac	6.3	5.9	0.7	0.07	0.15	0.02
West EQ Pac	13.0	12.6	2.0	0.23	0.36	0.05
SP STPS	8.3	6.4	1.0	0.07	0.08	0.01
NA SPSS	22.4	19.7	1.0	0.25	0.12	0.01
NA STSS	7.4	5.2	0.6	0.10	0.10	0.02
NA STPS	5.2	5.6	0.4	0.09	0.06	0.01
EQ Atl	8.8	6.5	0.6	0.07	0.06	0.01
SA STPS	9.7	8.5	0.5	0.10	0.06	0.007
IND STPS	11.1	10.6	1.0	0.04	0.10	0.01
SO STSS	5.9	12.4	2.0	0.14	0.08	0.01
SO SPSS	4.8	12.8	2.0	0.22	0.11	0.01
SO ICE	15.4	17.0	2.0	0.22	0.05	0.005

Supplementary Table 2: Twelve CMIP5 models included in analysis

Modeling Group	Model Name	Citation
Beijing Climate Center (BCC), China Meteorological Administration	BCC-CSM1.1m	Wu et al. 2012
Beijing Normal University (BNU), China College of Global Change and Earth System Science	BNU-ESM	Ji et al. 2014
Canadian Centre for Climate Modeling and Analysis, Victoria, BC	CanESM2	Chylek et al. 2011
National Center for Atmospheric Research, Boulder, CO, USA	CESM1-BGC	Lindsay et al. 2014
Centro Euro-Mediterraneo sui Cambiamenti Climatici, Lecce, Italy	CMCC-ESM	Fogli et al. 2009
NOAA Geophysical Fluid Dynamics Lab	GFDL-ESM2M	Dunne et al. 2012
Met Office Hadley Centre	HadGEM2	Collins et al. 2011
Institut Pierre-Simon Laplace, IPSL Climate Modelling Centre, France	IPSL-CM5-MR	Dufresne et al. 2013
Institute for Numerical Mathematics	INM-CM4	Volodin et al. 2010
Japan Agency for Marine-Earth Science and Technology, Atmosphere and Ocean Research Institute, The University of Tokyo	MIROC-ESM	Watanabe et al. 2011
Max-Planck-Institute for Meteorology	MPI-ESM-LR	Giorgetta et al. 2012a,b
Norwegian Climate Centre	NorESM1-ME	Tjiputra et al. 2012

Supplementary Table 3: Biome acronyms and long names (ref 32)

Biome acronym	Biome name
ICE	Marginal sea ice biome
SPSS	Subpolar seasonally stratified biome
STSS	Subtropical seasonally stratified biome
STPS	Subtropical permanently stratified biome
EQU	Equatorial biome

Supplementary Discussion

Assessement of modeled carbon cycle variability: Variability in CESM-LE modeled annual mean pCO_2 and CO_2 fluxes are compared to pCO_2 observations (Supplementary Table 1, left 3 columns) and to a CO_2 flux product derived from these same observations (Supplementary Table 1, right 3 columns). Within the uncertainty, modeled pCO_2 variance is correct in seven of the biomes, underestimated in 5 biomes and overestimated in 3 biomes.

However, in two of the three biomes where pCO_2 variability is overestimated by the model (SO STSS, SO SPSS), comparison to the CO_2 flux product suggests the model underestimates variability. In the third (NP STPS), the flux product comparison indicates that model appropriately simulates variability. Conversely, in the biomes where pCO_2 variability is underestimated, the CO_2 flux product comparison indicates either variability consistent with observations (NA STSS, EQ Atl), too high (NP STSS), or too low (NA SPSS, SA STPS). Similarly, in the biomes where pCO_2 variability is consistent with the observations, the CO_2 flux comparison indicates overestimation by the model (East Eq Pac, West Eq Pac, IND STPS), underestimation (NP SPSS, SO ICE), or consistency (SP STPS).

In the CESM-LE, pCO_2 variability is the dominant control on CO_2 flux variability[20]. Thus, the fact that these comparisons for pCO_2 and CO_2 flux variability differ significantly suggests that there is additional, unquantified uncertainty driven by the sparse sampling for pCO_2 and assumptions made in the development of the flux product[26]. That CESM-LE falls clearly within the range of observed pCO_2 and estimated CO_2 flux variability indicates that its modeled variability is, on the whole, consistent with our current observational understanding. More observations are needed to better constrain internal variability in the surface ocean carbon cycle.

Forced trends in the CMIP5 ensemble: Due to the combined effect of a smaller number of ensemble members for CMIP5 and the larger variability across these ensembles (Extended Data Fig 2d-f), due in part to structural differences[27], the forced trend in CO_2 flux cannot be identified from CMIP5 across in most of the global oceans, even for the timeframe 1990-2089 (Extended Data Fig 2a-c). Where the forced trend from CMIP5 is discernable, primarily in the equatorial Pacific and Southern Ocean, it is of the same sign as CESM-LE (increasing uptake) but of weaker magnitude.

Supplementary references:

31. Bakker, D. C. E., Pfeil, B., Smith, K., Hankin, S., Olsen, A., Alin, S. R., Cosca, C., Harasawa, S., Kozyr, A., Nojiri, Y., O'Brien, K. M., Schuster, U., Telszewski, M., Tilbrook, B., Wada, C., Akl, J., Barbero, L., Bates, N. R., Boutin, J., Bozec, Y., Cai, W. J., Castle, R. D., Chavez, F. P., Chen, L., Chierici, M., Currie, K., de Baar, H. J. W., Evans, W., Feely, R. A., Fransson, A., Gao, Z., Hales, B., Hardman-Mountford,N. J., Hoppema, M., Huang, W.-J., Hunt, C. W., Huss, B., Ichikawa, T., Johannessen, T., Jones, E. M., Jones, S. D., Jutterström, S., Kitidis, V., Körtzinger, A., Landschützer, P., Lauvset, S. K., Lefèvre, N., Manke, A. B., Mathis, J. T., Merlivat, L., Metzl, N., Murata, A., Newberger, T., Omar, A. M., Ono, T., Park, G.-H., Paterson, K., Pierrot, D., Rios, A. F., Sabine, C. L., Saito, S., Salisbury, J., Sarma, V. V. S. S., Schlitzer, R., Sieger, R., Skjelvan, I., Steinhoff, T., Sullivan, K. F., Sun, H., Sutton, A. J., Suzuki, T., Sweeney, C., Takahashi, T., Tjiputra, J., Tsurushima, N., van Heuven, S. M. A. C., Vandemark, D., Vlahos, P., Wallace, D. W. R., Wanninkhof, R., and Watson, A. J.: An update to the Surface Ocean CO2 Atlas (SOCAT version 2), Earth System Science Data, 6, 69–90, doi:10.5194/essd-6-69-2014, URL: http://www.earth-syst-sci-data.net/6/69/2014/, 2014.

32. Fay, A. R., & McKinley, G. A. (2014). Global open-ocean biomes: mean and temporal variability. *Earth System Science Data*, *6*(2), 273-284.

33. Fay, A. R., McKinley, G. A., & Lovenduski, N. S. (2014). Southern Ocean carbon trends: Sensitivity to methods. *Geophysical Research Letters*, *41*(19), 6833-6840.

34. Chylek, P., Li, J., Dubey, M. K., Wang, M., and Lesins, G. Observed and model simulated 20th century Arctic temperature variability: Canadian Earth System Model CanESM2, *Atmos. Chem. Phys. Discuss.,* **11,** 22893-22907 (2011).

35. Collins, W. J., et al. Development and evaluation of an Earth-system model – HadGEM2, *Geoscientific Model Development* **4.4** 1051-1075 (2011).

36. Dufresne, J-L., M-A. Foujols, Sébastien Denvil, Arnaud Caubel, Olivier Marti, Olivier Aumont, Y. Balkanski et al. :Climate change projections using the IPSL-CM5 Earth System Model: from CMIP3 to CMIP5. *Climate Dynamics* 40, no. 9-10 (2013): 2123-2165.

37. Dunne, J. P. et al. GFDL's ESM2 global coupled climate-carbon Earth System Models Part I: Physical formulation and baseline simulation characteristics. *Journal of Climate*. **25** 6646-6665 (2012).

38. Fogli, P. G., Manzini, E., Vichi, M., Alessandri, A., Patara, L., Gualdi, S., ... & Navarra, A. (2009). INGV-CMCC carbon (ICC): a carbon cycle earth system model. *CMCC Research Paper*, (61).

39. Giorgetta, M., et al. CMIP5 Simulations of the Max Planck Institute for Meteorology (MPI-M) Based on the MPI-ESM-LR Model: The Historical Experiment, Served by ESGF, *World Data Cent. for Clim*, (2012a).

40. Giorgetta, M., et al. CMIP5 Simulations of the Max Planck Institute for Meteorology (MPI-M) Based on the MPI-ESM-LR Model: The rcp85 Experiment, Served by ESGF, *World Data Cent. for Clim*,(2012b).

41. Ji, D., L. Wang, J. Feng, Q. Wu, H. Cheng, Q. Zhang, J. Yang, W. Dong, Y. Dai, D. Gong, R.-H. Zhang, X. Wang, J. Liu, J. C. Moore, D. Chen, and M. Zhou (2014). Description and basic evaluation of Beijing Normal University Earth System Model (BNU-ESM) version 1. *Geosci. Model Dev*., 7, 2039–2064.

43. Lindsay, K., et al. Preindustrial-control and twentieth-century carbon cycle experiments with the Earth System Model CESM1 (BGC). *Journal of Climate* **27**.24 8981-9005 (2014).

45. Tjiputra J. F., et al..Evaluation of the carbon cycle components in the Norwegian Earth System Model (NorESM), *Geosci. Model Dev.*, **6.**2, 301-325. (2012)

46. Volodin E. M., Dianskii, N. A. and Gusev, A. V. Simulating Present-Day Climate with the INMCM4.0 Coupled Model of the Atmospheric and Oceanic General Circulations. *Izvestiya, Atmospheric and Oceanic Physics*, **46**, 414-431, (2010).

47. Watanabe, S., et al. MIROC-ESM 2010: model description and basic results of CMIP5-20c3m experiments, *Geosci. Model Dev.,* **4**, 845-872, (2011).

48. Wu, T. The 20th century global carbon cycle from the Beijing Climate Center Climate System Model (BCC CSM). *Journal of Climate* (2012).

Extended Data for

Detectability of change in the ocean carbon sink

Galen A. McKinley, Darren J. Pilcher, Amanda R. Fay, Keith Lindsay,

Matthew C. Long, Nicole S. Lovenduski

Figure Captions:

Extended Data Figure 1. Comparison of 1982-2011 mean CO_2 flux (molC/m^2/yr): **a** Data-based climatology, (Landschützer et al. 2014), **b** CESM large ensemble 32-member mean, and **c** mean of 12 CMIP5 models.

Extended Data Figure 2. Forced trends and internal variability of CMIP5 trends in sea-to-air CO_2 flux (molC/m^2/yr^2). Forced trends for **a** 1990-1999, **b** 1990-2019 and **c** 1990-2089. Gray is where the forced trend cannot be distinguished from the variability with 95% confidence (Methods). CO_2 flux trend standard deviations, indicating the impact of internal variability on CO_2 flux trends, for **d** 1990-1999, **e** 1990-2019, **f** 1990-2089. Negative indicates increasing ocean carbon uptake.

Extended Data Figure 1

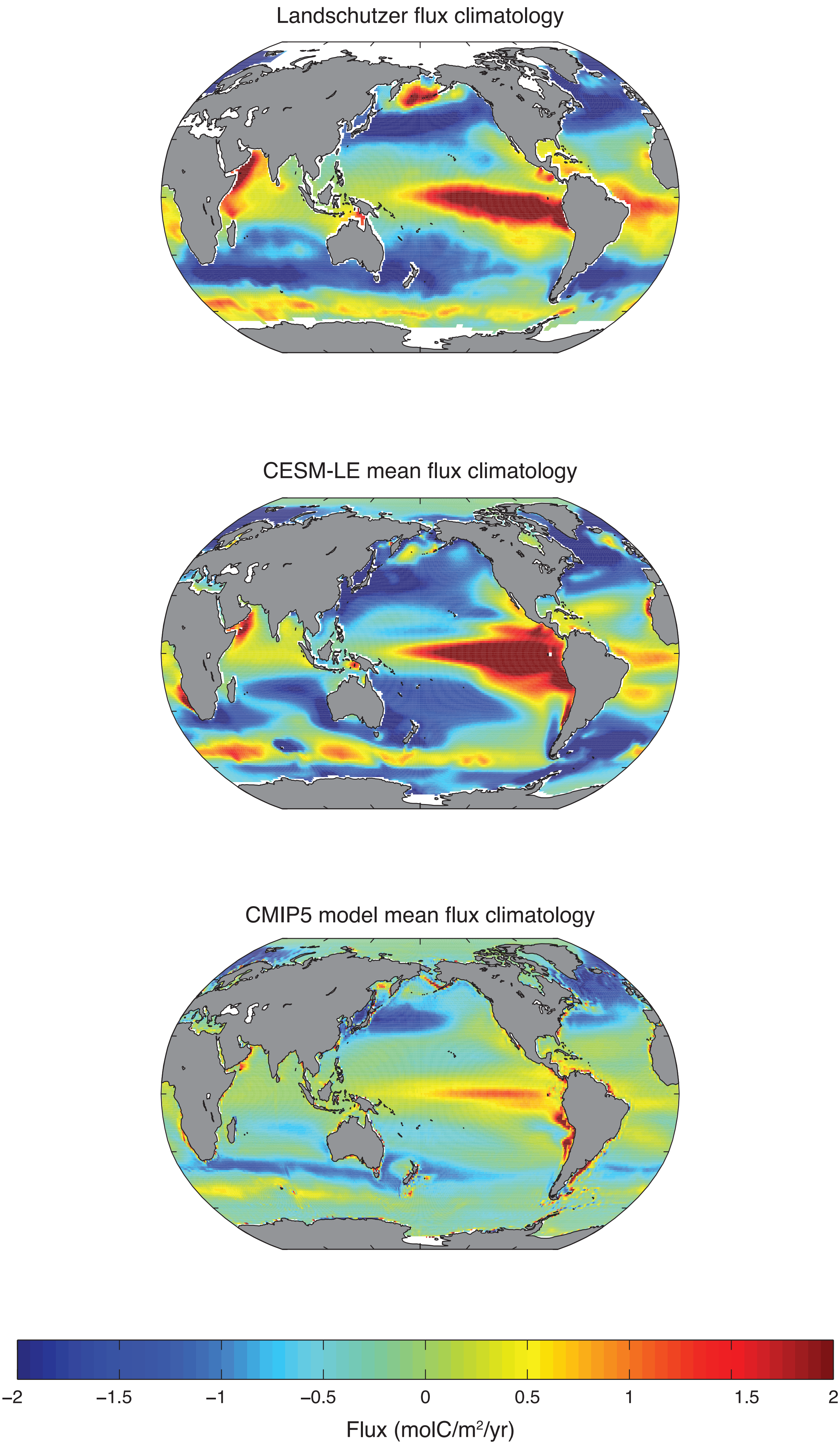

Extended Data Figure 2